

NEW METHOD

Rapid-Motion-Perception Based Cardiac Navigators: Using the High Flow Blood Volume as a Marker for the Position of the Heart

Vinay M. Pai, Ph.D.,^{1,*} and Han Wen, Ph.D.²

¹Department of Radiology, New York University School of Medicine, New York, New York, USA

²Laboratory of Cardiac Energetics, National Institutes of Health, National Heart, Lung and Blood Institute, Bethesda, Maryland, USA

ABSTRACT

Navigators have been developed as one of the many approaches to reducing motion artifacts due to respiration. A typical navigator approach applies a pencil-beam style profile crossing the diaphragm to track the superior-inferior (SI) motion of the diaphragm, and subsequently applying correlations to determine the heart location. This approach necessitates a priori knowledge of the correlation coefficients between heart and diaphragm motion, a variable parameter among patients. This paper presents an alternative navigator method based on Rapid Motion Perception (RaMP). This method acquires profiles of the ventricular blood volume based on its high flow velocity. The position of the blood volume is a direct representation of the position of the heart. This method allows cardiac navigation in two orthogonal directions simultaneously, eliminates the need to obtain correlations to the diaphragm motion, and increases tracking reliability for individual patients. A prospective version of RaMP navigators has been implemented on a clinical 1.5 T scanner, and preliminary tests on human volunteers show that this method can successfully track the heart position over the entire respiratory period. This navigation scheme is tested for predicting superior-inferior and anterior-posterior (AP) motion of the heart for breath-hold and free breathing conditions. Bland-Altman plots comparing the motion predicted by the navigators and that computed from single-shot images immediately following the navigators, show that the accuracy of this method is ± 1.43 mm in the SI direction and ± 0.84 mm in the AP direction. The RaMP navigator is suited for real-time tracking of the bulk translational motion of the heart.

Key Words: Navigators; MRI; Cardiac tracking; Complex difference; Blood flow; Slice-tracking; Motion.

*Correspondence: Vinay M. Pai, Ph.D., Department of Radiology, New York University School of Medicine, 650 First Avenue, Room 611, New York, NY 10016, USA; E-mail: vinay.pai@med.nyu.edu.



INTRODUCTION

Cardiac imaging sequences often span multiple heartbeats to obtain temporal and spatial resolutions. Under such conditions, respiratory motion can significantly impair the quality of magnetic resonance (MR) images with motion artifacts.

A number of techniques have been proposed and developed over the years to minimize the effects of respiration on MR images. Breath-hold techniques (Duerinckx and Urman, 1994; Manning et al., 1993; Meyer et al., 1992; Paling and Brookeman, 1986; Pennell et al., 1993; Post et al., 1995; Sakuma et al., 1994) and navigator echoes (Ehman and Felmler, 1989; Haacke et al., 1995; Hofman et al., 1995; Sachs et al., 1994; Wang et al., 1996), both prospective and retrospective, are among the approaches that have been developed. Each of these techniques has its capabilities and limitations. While breath-holding is the most commonly used approach to reducing motion artifacts, it limits the available scan time and may cause physiological changes during the course of a breath-hold.

Navigator methods, on the other hand, allow normal or quiet breathing and require less patient coaching. They extend the available scan time greatly and maintain a normal physiological state. However, it is often difficult to accurately measure the position of the heart in real time.

One approach has been locating the position of the diaphragm of the patient at its interface with the lungs, and utilizing this information to determine the current position of the heart, in order to prospectively or retrospectively apply a motion correction to the imaging slice. This approach, however, requires knowledge of correlations between the motion of the diaphragm and the cardiac movement. It has been shown (Wang et al., 1995) that the respiratory motion of the heart is approximately a global translation, with the motion being dominated by the superior-inferior (SI) component and approximately, linearly correlated to the SI motion of the diaphragm. The mean correlating factors for the right coronary artery (RCA) root and the left anterior descending (LAD) artery vis-à-vis the SI position of the diaphragm were determined to be 0.57 ± 0.26 [standard deviation (SD)] and 0.70 ± 0.18 (SD), respectively (Wang et al., 1995).

However, subsequent work (Danas et al., 1999; Johansson et al., 1998; Keegan et al., 2002; Nagel et al., 1999; Nehrke et al., 2001; Taylor et al., 1998) has also showed varying amount of bulk heart motion in the anterior-posterior (AP) direction, and considerable variation in the correlating factors among individuals, which would necessitate determining correlating factors

for each patient, if diaphragm-based navigator positions are used for correctly positioning imaging slices. Application of navigators to the free wall of the left ventricle (LV) is more reliable, but has the disadvantage that magnetization voids can occur at the lung-LV free wall interface (Haacke et al., 1995; Wang et al., 1996), and the navigator signal-to-noise ratio (SNR) can be considerably reduced due to the smaller diameters of the navigator beams at such locations (Stuber et al., 1999). Application of pencil-beam navigators directly through the heart (Danas et al., 1999; Johansson et al., 1998) can generally lead to destructive interference between the pencil beam navigators and the imaging volume, affecting image quality and navigator accuracy (Nehrke et al., 2001).

In the present article, an alternative navigator approach is presented, in which, instead of tracking the motion of the diaphragm or the LV free wall, the fast-flowing blood volume in the heart is tracked during the cardiac cycle. Due to its sensitivity to high velocity flow, the approach is called Rapid Motion Perception (RaMP) navigator. In this approach, during systolic emptying (or diastolic filling), the fast-moving blood volume in the ventricles is isolated by performing a complex difference analysis of the flow-sensitized profiles. This complex difference analysis suppresses the stationary or slow-moving spins. Simultaneous tracking of SI and AP movement of the heart is demonstrated by this approach. Small flip angle excitations gave sufficient SNR without creating saturation effects.

THEORY

RaMP Overview

During systolic emptying (or diastolic filling), the position of the fast-flowing ventricular blood volume can be used as a marker for the position of the heart. The profile of this blood volume can be obtained by a complex difference analysis of one-dimensional, flow-sensitized data through the application of velocity-encoding bipolar gradients during the navigator.

Figure 1a shows the RaMP navigator sequence. This method essentially uses a series of spoiled Fast Low Angle SHot (FLASH) echoes (Crawley and Henkelman, 1987; Haase et al., 1986) and incorporates an alternating pair of bipolar velocity-encoding gradients. If $M_{1,k}$ and $M_{2,k}$ represent the transverse magnetization at the readout after the first and second bipolar gradients, respectively, for the k th navigator echo, then the complex



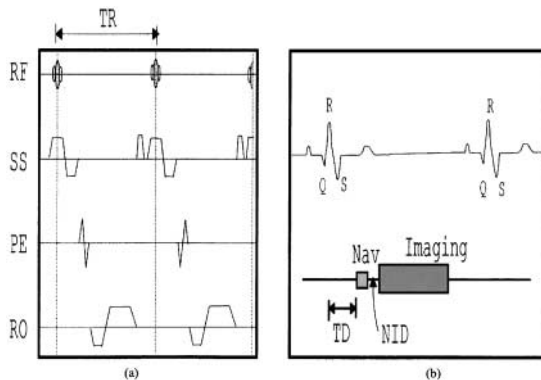


Figure 1. Flow-sensitive navigators (RaMP) scheme. (a) RaMP is comprised of a spoiled-FLASH sequence with alternating bipolar velocity-encoding gradients. TR is the repetition time between successive application of RF pulses. The figure illustrates velocity encoding along the phase-encode (PE) direction. SS represents the slice-select direction and RO is the readout direction. (b) Location of the RaMP (Nav) vis-à-vis the imaging sequence. NID is the Navigator-Imaging Delay time, while TD is the trigger delay.

difference for the RaMP scheme (CD) is given by

$$CD = |M_{2,k} - M_{1,k}| \quad (1)$$

where the transverse magnetization values are obtained by performing a one-dimensional Fourier Transform (FT) on the raw data along the readout, or frequency-encoding, direction.

The first cardiac cycle scan is considered as the reference scan and establishes the reference position of the heart. The CD profile of the blood volume for this cycle is used as the reference profile. This reference profile is then compared with the CD data of subsequent scans to determine their offsets from the reference position. Mathematically, this comparison is realized with standard motion analysis by profile correlation (Ehman and Felmlee, 1989), detailed below.

1. A reference profile is first obtained for the reference scan. This is done by performing the following operations on the reference CD profile:

- Fast-Fourier Transforming (FFTing) the magnitude of the data.
- Applying a Fermi filter to remove any high frequency noise in the profile.
- Zero-filling the filtered data and applying an inverse FFT to obtain an interpolated profile.
- Finally, a thresholding operation is performed on this data to yield the one-dimensional reference profile.

2. For profile correlation of the CD data of the subsequent scans with the reference, the following operations are then performed:

- The magnitude of the CD data for subsequent scans is FFTed.
- This is then zero-filled, flipped about its midpoint, and multiplied with the Fourier transformation of the reference profile.
- Application of an FFT operation to this product yields the sliding correlation among the profiles. The amount of shift that results in the maximum correlation value is used as the position shift in subsequent scans.

RaMP Guided Imaging

Figure 1b shows the arrangement for RaMP guided imaging. This sequence is electrocardiographically gated (ECG-gated), and a trigger delay (TD) is used to locate the RaMP in mid-systole to obtain the maximum flow signal. The RaMP data are analyzed in real time and the position corresponding to the motion of the heart is computed during the time delay between the navigators and the imaging sequence (navigator–imaging delay, NID). Typical numerical values for all the delay times are presented in the Methods section. The slice shift corresponding to the position change is applied during the NID and the imaging scan is then played out.

METHODS

All the scans were performed on a Siemens Sonata 1.5 T whole-body clinical scanner [Siemens Medical Systems (SMS), Iselin, NJ], with a gradient set of 40 mT/m and maximum slew rates of 200 mT/m-ms. As mentioned earlier, the navigators were ECG-triggered, spoiled-FLASH echoes with the gradient spoiling in the Slice-Select direction, and included alternating pairs of bipolar, velocity-encoding gradients. For a given pair of RaMP echoes, each half (comprising of one bipolar encoding gradient) was implemented with a repetition time (TR) of 8 ms and an echo time (TE) of 3.5 ms, RF flip angle (α) of 10° and slice thickness of 20 mm. Thus, a pair of RaMP echoes along a single axis, yielding the cardiac position shift along that direction, would occupy 16 ms time duration in a cardiac cycle. The pulse sequence permits obtaining the navigator information in all three dimensions [superior-inferior (SI), anterior-posterior (AP), and left-right (LR)].



The imaging sequence following the navigators was a single-shot Fast Imaging with Steady Precession (FISP) sequence (Oppelt et al., 1986) whose implementation had a TR/TE/ α of 3.2/1.6/30°, and slice thickness of 8 mm. The base resolution for the image matrix and the navigator echoes was 256 pixel, while the field-of-view (FoV) along the readout direction was 340 mm, which implied a linear resolution of 1.328 mm/pixel for both the navigator echoes and the imaging data. The imaging sequence included eight dummy cycles played out at the start of the imaging scan for bringing the transverse magnetization to steady-state.

An ECG-prospectively triggered FLASH single-slice, multiphase breath-hold cine sequence (cine TurboFLASH; Siemens Medical Systems) with a TR/TE/ α of 27/3.4/20° was used to determine the time to mid-systole for each human volunteer who participated in the navigator study. This time was used to determine the trigger delay time for the RaMP echoes. Typically, the TD time was 159 ms \pm 13 ms, while the navigator-imaging delay (NID) was 1.4 ms.

Ten normal volunteers (age range: 21–55 years, mean age: 35 years, 6 males, 4 females) were scanned with a phased array surface coil within all guidelines of human subject research of the National Institutes of Health. The scanning process utilized the following protocol:

1. ECG-gated FLASH multislice multi-axis non-breath-hold localizers (TurboFLASH; SMS) were used to localize the heart.
2. Three-dimensional local volume-of-interest field shims were calculated with a manufacturer-supplied shimming sequence.
3. The approximate time to mid-systole was determined by applying the cine sequence indicated above.
4. RaMP echoes were applied, followed by the imaging sequence, under free-breathing and breath-hold conditions.

Steps 1 through 3 were performed only at the start of the experiment to set up the parameters for the execution of the final step.

For verification of the method, the heart motion as tracked by the imaging sequence was compared to the motion predicted by the RaMP scheme to determine the reliability of the navigators. In case of the images obtained from the imaging sequence, the imaging scan for the first cardiac cycle was used as a reference image. Imaging scans for subsequent cardiac cycles were correlated to this reference image by the following process:

1. A rectangular region-of-interest (R-ROI) was drawn to include the heart and surrounding organs, in the first imaging scan (the reference scan), and propagated through the examination image stack.
2. A ROI was drawn around the heart (H-ROI) in the R-ROI of the first imaging scan to develop a positive mask.
3. A negative mask was applied on the chest wall (C-ROI) to minimize the position shift error that can occur when the chest wall has a very high signal level. This was done by creating a mask by drawing an ROI around the chest wall, and subtracting this mask from all the images in the exam stack. The entire image stack was subsequently visually examined to ensure that the negative mask did not intrude onto the H-ROI.
4. A two-dimensional extension of the one-dimensional correlation approach discussed above, was performed between the H-ROI mask and the R-ROIs in subsequent imaging scans. This approach yields the position shift of the heart in the SI and AP directions in each imaging scan.
5. The images in the stack subsequently were also examined visually by applying the position shift values, to ensure that the position shifts were correctly calculated.

The implementation of the prospective approach of RaMP on the scanner was done as per Fig. 2. For navigating only in one dimension, two RaMP echoes are acquired, i.e., a pair of alternating bipolar gradients, while four echoes are needed for navigating in two dimensions. The navigator projection data is processed in real time using a site-developed reconstruction package (utilizing the algorithm detailed above), and the displacement information obtained is used to translate the imaging slice before running the imaging sequence. For the two prospectively corrected cases (Case I and Case II) presented in this paper, a two-dimensional version of RaMP was implemented, i.e., motion correction was applied only in the SI and AP directions. The flow encoding was done in the LR direction. Both the navigating and the imaging slices were sagittal in orientation. For Case I, an agarose-filled tube was placed above the phased-array surface coil to track the motion shift predicted by the navigator echoes; the body coil was used as the receiver in this case. For Case II, the phased-array surface coil was used as the receiver.



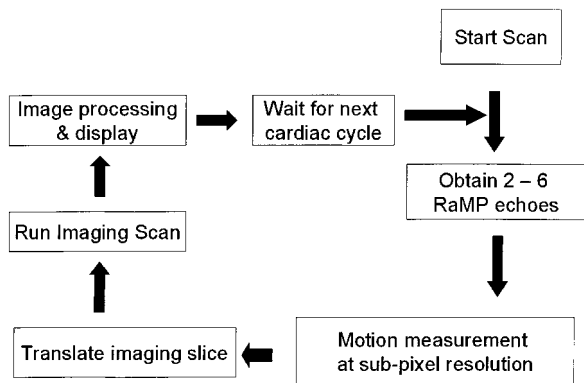


Figure 2. Block diagram illustrating the implementation of prospective RaMP. For one-dimensional navigating, two RaMP echoes are acquired, and for three-dimensional navigating, six echoes are acquired.

RESULTS

It has been well established (Wang et al., 1995) that the cardiac movement in the thorax is dominated by the superior-inferior (SI) motion, with the anterior-posterior motion being a fraction of the SI motion. Although LR motion of coronary arteries may be significant (Keegan et al., 2002), RaMP did not observe appreciable LR bulk motion of the heart when compared with AP and SI motion. Therefore, the movement of the coronary vessels

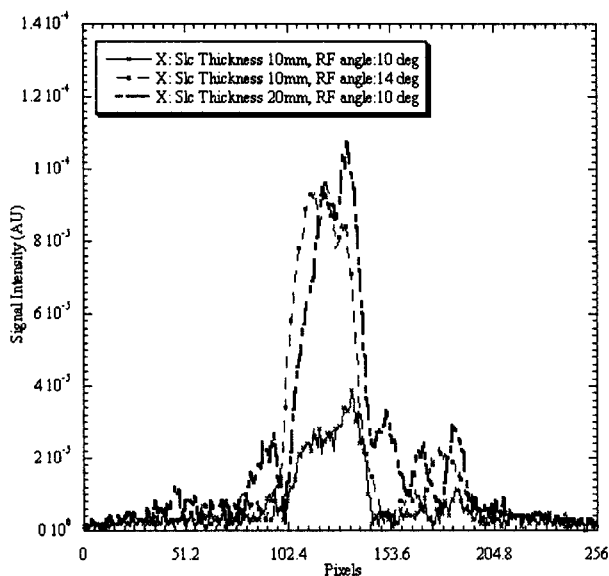
are likely the result of deformation of the heart, and RaMP is inherently insensitive to deformation and limited in this respect. In this paper we focus on the AP and SI bulk translational motion, and a sagittal slice is excited to detect these components.

It should be noted here, though, that RaMP navigators, in principle, can track all three directions of global cardiac motion, and prospectively slice-shift in response to movement in any or all of the three directions.

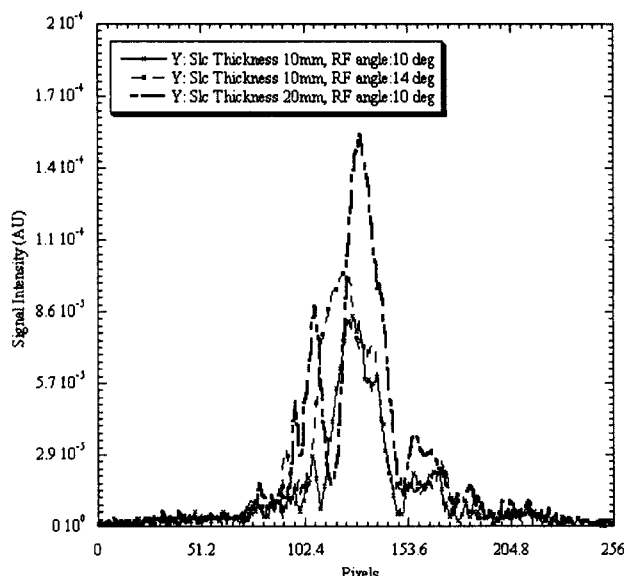
Feasibility Studies

In order to verify the capability of the RaMP navigators to predict cardiac displacement and determine the resolution range, the feasibility stage consisted of comparing the displacements predicted by the RaMP navigators in the SI and AP directions with that determined from the images obtained with the imaging sequence under a nonprospective implementation. Bland-Altman plots (Bland and Altman, 1986; 1999) are also obtained to determine the 95% limits of agreement, estimated by mean difference \pm 2 standard deviation of the differences, between the measurements by the two approaches.

Also, in order to determine the variation in navigator signal intensity with respect to slice thickness, a single volunteer comparison study was performed with



(a) Projection along SI direction.



(b) Projection along AP direction.

Figure 3. Signal intensity variation with navigator slice thickness and RF flip angle.



navigator slice thicknesses of 10 mm and 20 mm and RF flip angles of 10° and 14° . Figure 3 shows the signal intensity comparison for one projection along the SI and AP directions respectively. It is obvious from these plots that for tracking the SI projections, one could use a

thinner slice with a higher flip angle (10 mm and 14°) and achieve signal intensity levels comparable to that obtained by using a thicker slice at 10° . However, even at a 14° flip angle, the signal intensity along the AP direction for the thinner slice is much reduced compared

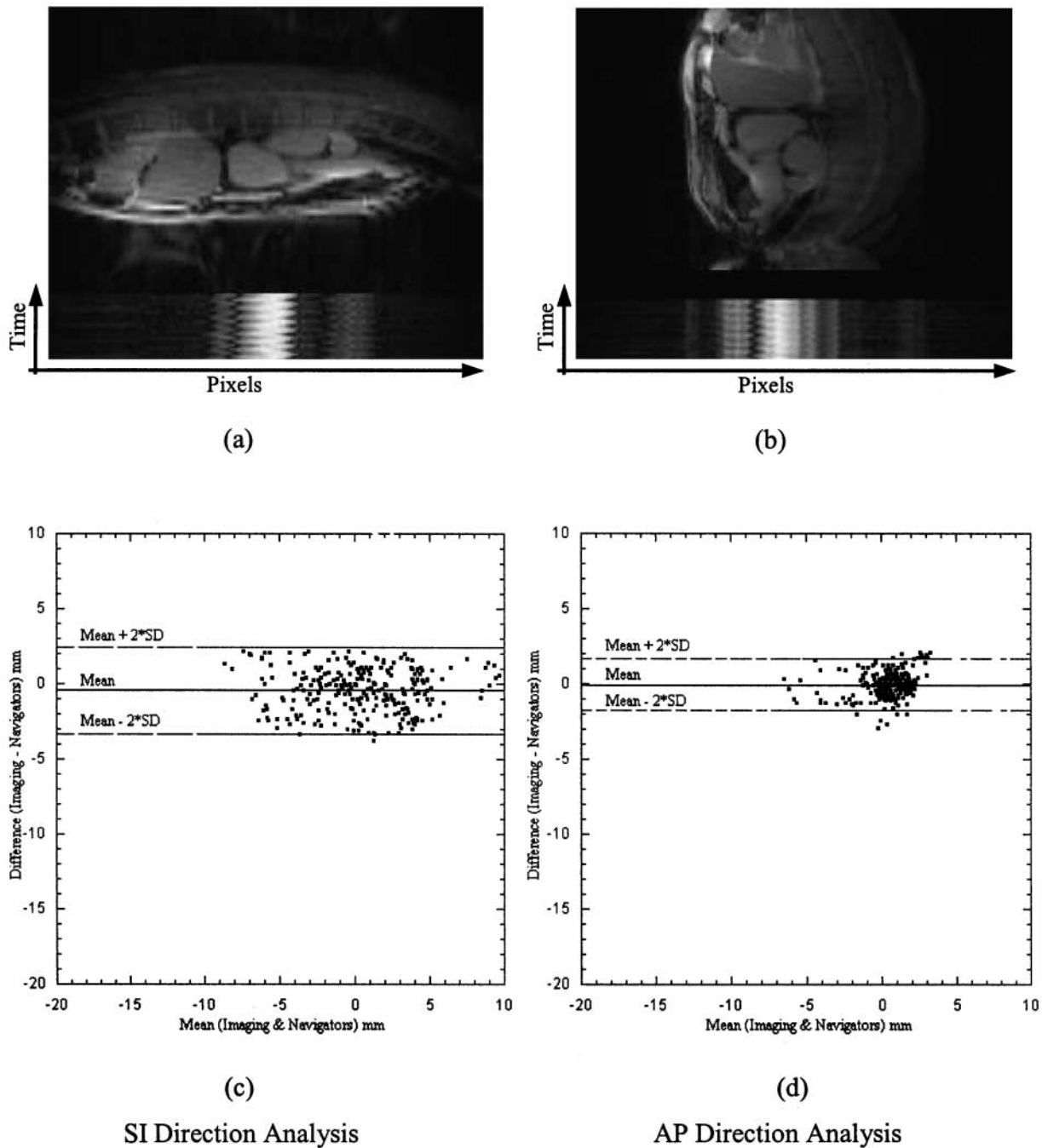


Figure 4. Top (a and b): SI and AP direction navigator echoes for free-breathing conditions for a single volunteer, with an overlay of the corresponding imaging scan. Bottom (c and d): Bland-Altman plots for the data obtained in the SI and AP directions, respectively, from 10 volunteers under free-breathing conditions.

to that obtained by using the thicker slice at 10° . Thus, under conditions where the SI and AP motion need to be tracked, care needs to be taken to ensure that the proper combination of slice thickness and RF flip angle is used to obtain high SNR for successful use of navigator echoes. A detailed optimization analysis using multiple

volunteers is currently under way to determine the most suitable range of slice thickness and flip angles for the technique to work successfully.

Two different cases were considered during the feasibility study. In the first case, the volunteers were allowed to breathe freely during the entire scan, which

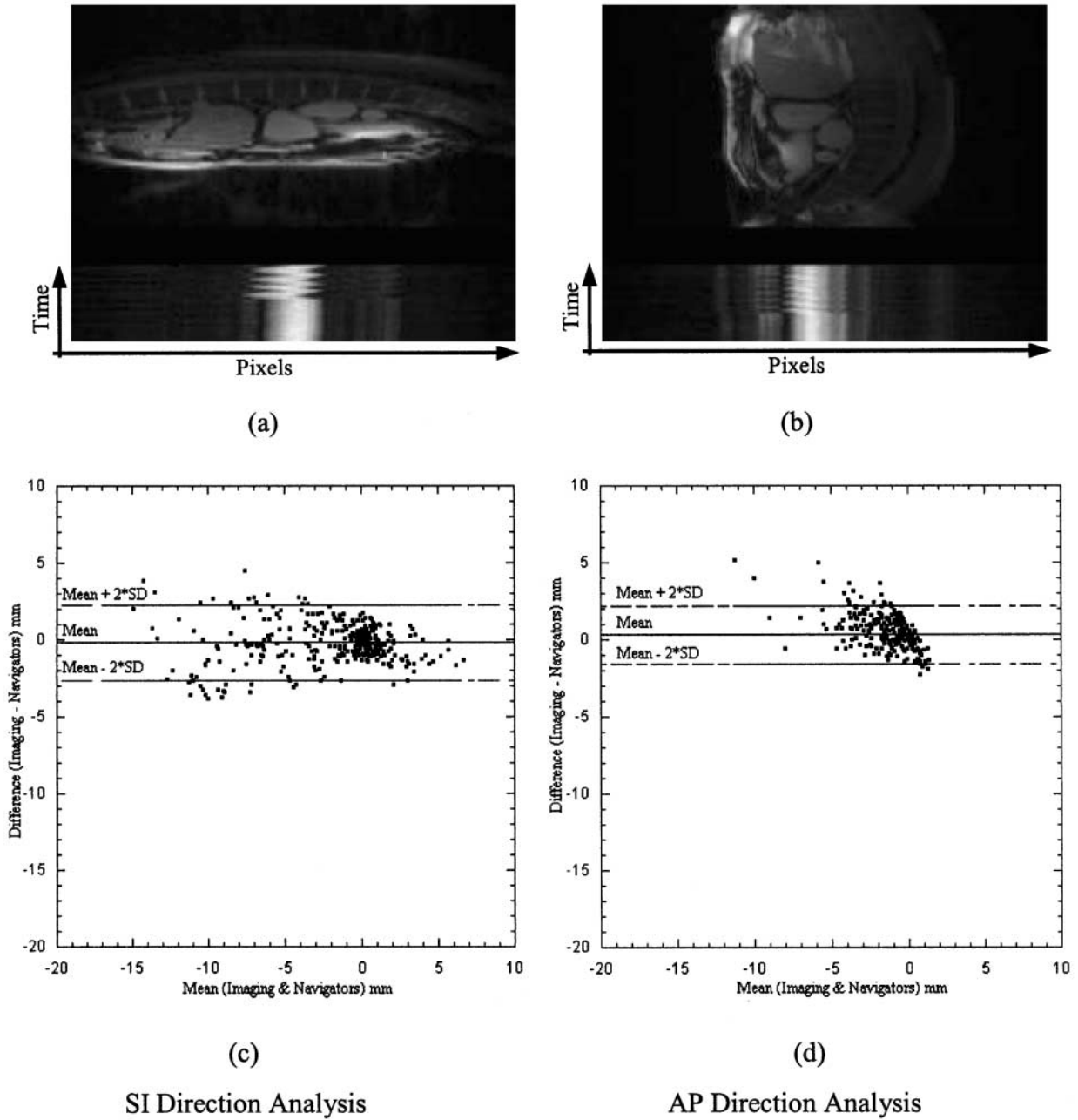


Figure 5. Top (a and b): SI and AP direction navigator echoes for breathhold and subsequent free-breathing conditions for a single volunteer, with an overlay of the corresponding imaging scan. Bottom (c and d): Bland-Altman plots for the data obtained in the SI and AP directions, respectively, from 10 volunteers under similar conditions.



lasted for 29 sec, and in the second case, the volunteers were made to hold their breath at the start of the scan, and then asked to release their breath 10 to 15 sec into the scan, which lasted for a total duration of 44 sec. The second case was considered in order to obtain a wider range of breathing displacements than would be obtained typically in a free-breathing scenario.

1. Case I: The RaMP navigators' prediction capability along the SI and the AP directions for the free-breathing condition is illustrated in Fig. 4. Figures 4a and 4b show the RaMP CD navigators for the SI and AP directions respectively. Imaging scan snapshots (time $t = 0$) are overlaid above the navigator echoes to provide approximate indicators of the location of the maximal

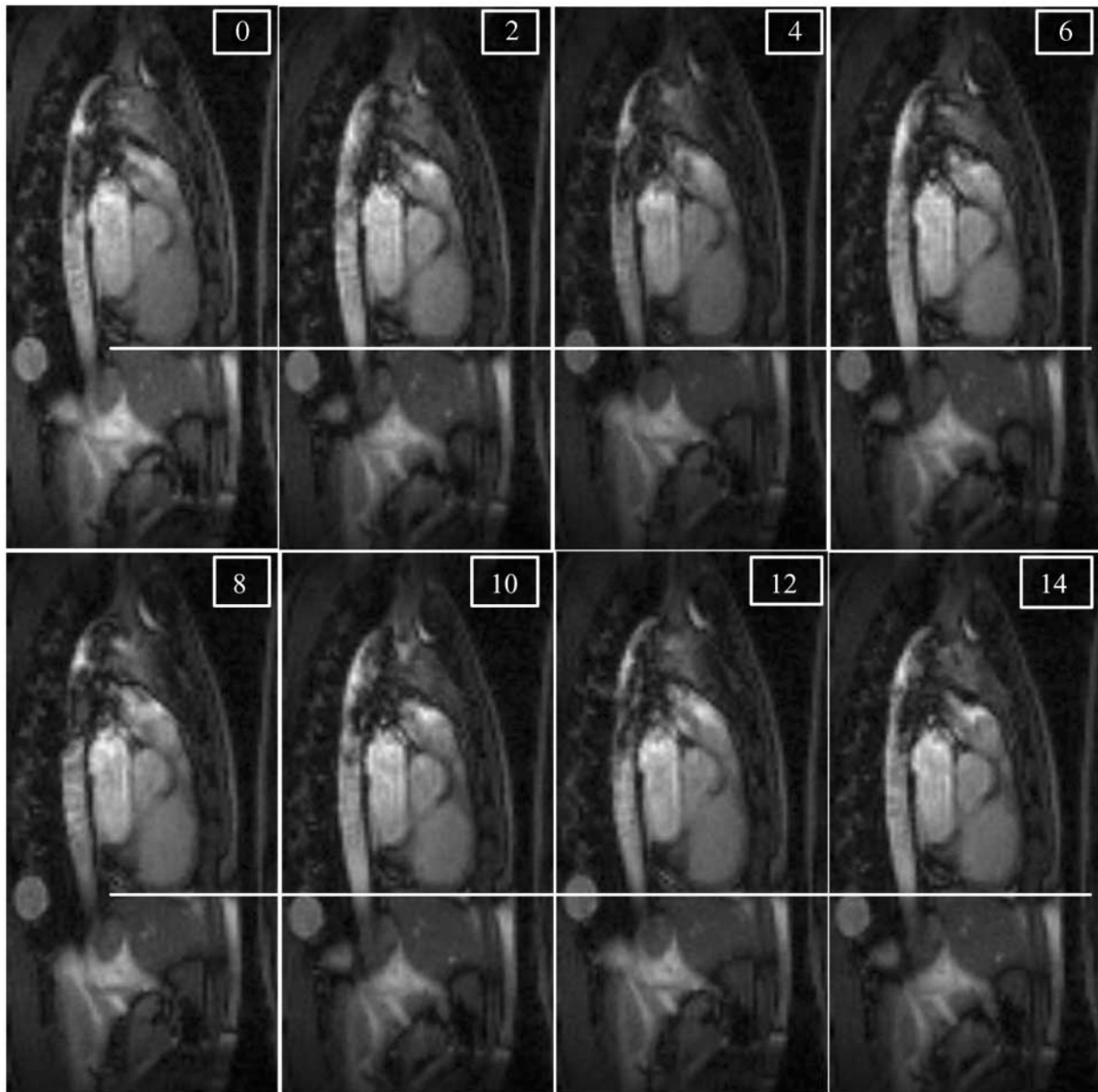


Figure 6. Prospectively navigated imaging scans for Case I (see text) over 15 cardiac cycles. Every other cardiac cycle image is shown to ensure clarity. The marker line is provided to illustrate the stationary nature of the heart, and the motion of the imaging slice can be tracked by monitoring the displacement of the agarose tube phantom in the left-inferior section of the images.

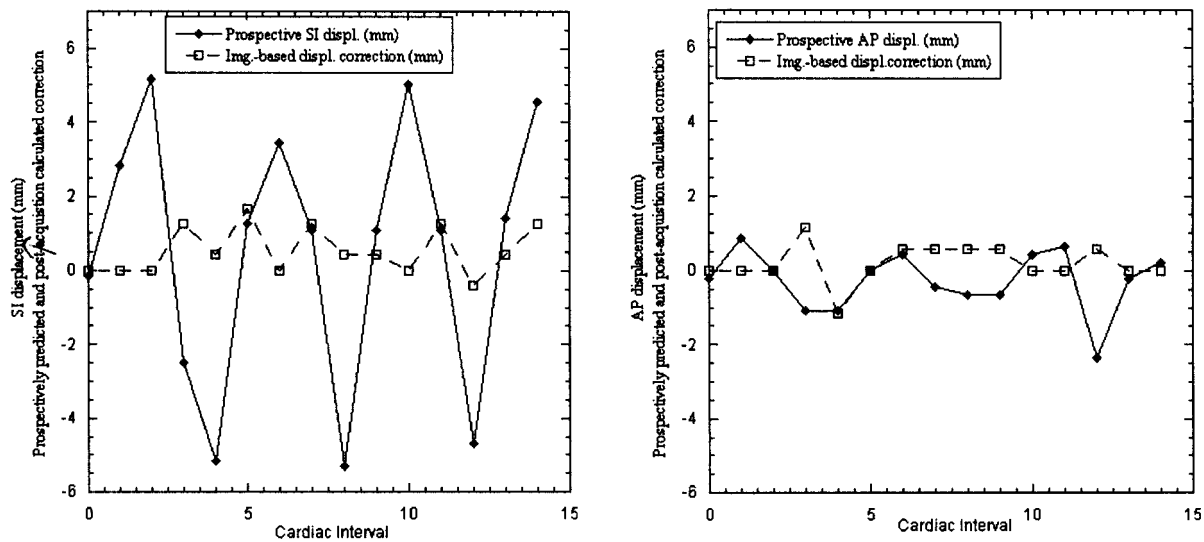


Figure 7. SI and AP motions as predicted by the navigators and displacement corrections needed, as per postprocessed, prospectively aligned images, for Case I.

navigator signal. In both cases, the RaMP signal is dominated by the ventricular blood volume. The oscillation in the signal corresponds to the motion of the heart under free-breathing conditions.

Figures 4c and 4d show the Bland-Altman plots for the SI and AP directions respectively. In these plots, the cardiac position shifts as predicted by the RaMP navigators were compared to that observed in the images obtained through the imaging scan, for the 10 volunteers examined. For both the SI and AP measurements, there is a bias [less than 1 standard deviation (SD)] of the navigator measurements as compared with the imaging measurements, namely 0.44 and 0.06 mm, respectively. The lower and upper 95% acceptance bounds are 3.30 and 2.41 mm for the SI measurements and -1.75 and 1.63 mm for the AP measurements.

2. Case II: As mentioned earlier, in this case, the volunteers held their breath at the beginning of the scan, and released the breath-hold 10–15 sec into the scan. This provided a wider range of respiratory motion in an individual, and among individual volunteers. Figure 5 illustrates the behavior of the RaMP navigators in the SI and AP directions under such conditions. Figures 5a and 5b show the navigator echoes, while Fig. 5c and 5d show the Bland-Altman plots. As in the free-breathing case, the imaging scan snapshots overlaid above the navigator echoes were taken at the start of the scan, and thus can only provide an approximate indication of the location of the maximal navigator signal. From the echoes, it is self-evident that the ventricular blood volume remains almost stationary during the breath-

hold condition, and undergoes relatively large displacements in both the directions considered, when the volunteer resumes free breathing.

From the Bland-Altman plots, it is obvious that there is a wide range in the respiratory motion in the volunteer base considered, when they are coming out of the breath-hold condition. For these cases, the bias of the navigator measurements as compared with the imaging measurements was -0.20 mm in the SI direction, and 0.33 mm in the AP direction. The lower and upper 95% acceptance bounds were -2.65 and 2.26 mm in the SI direction and -1.54 and 2.20 mm in the AP direction.

From these cases, the accuracy of the RaMP approach in predicting bulk motion is determined to be ± 1.43 mm in the SI direction and ± 0.84 mm in the AP direction during normal breathing.

Prospective Application

Having established the feasibility of the RaMP navigators to predict the cardiac displacement, the prospective approach was implemented on the clinical scanner as outlined earlier. Figures 6 and 8 show the RaMP implementation on two different human volunteers. While the prospective scans were done over 15 cardiac cycles, for the purpose of clarity, the figures show the cardiac position over every other cardiac cycle. Marker lines are drawn through the figures to illustrate the shift in position of the various organs, and the absence of heart motion.



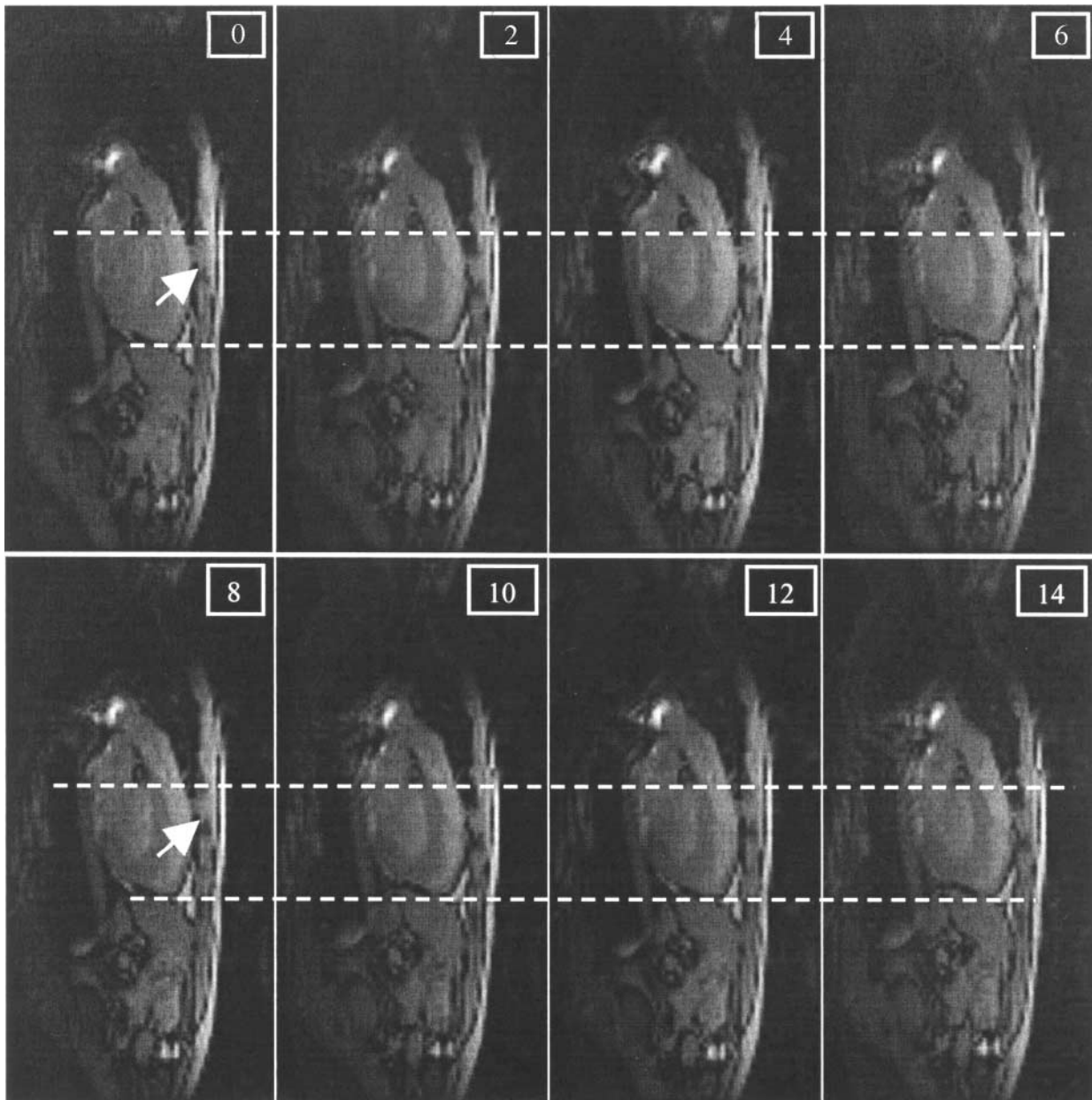


Figure 8. Prospectively navigated imaging scans for Case II (see text) over 15 cardiac cycles. Every other cardiac cycle image is shown to ensure clarity. The marker lines illustrate the stationary nature of the heart, and the displacement of the chest wall due to the motion of the imaging slice. The reader can track the “notch” in the chest wall as indicated by the arrows in cycle zero and cycle eight in combination with the upper marker line to monitor the chest wall displacement. The lower marker line indicates the stationary position of the left ventricle wall.

In Case I (Fig. 6), as mentioned earlier, an agarose-filled tube was placed above the phased-array surface coil, in order to track the motion correction determined from the RaMP implementation. The marker line drawn through the apex of the heart clearly shows the motion of the tube and the various organs, and also shows that the

heart appears stationary during the entire imaging cycle (15 heartbeats).

In order to determine the accuracy of the prospective navigation, the prospectively aligned images were postprocessed to determine whether there was any displacement correction required between the successive

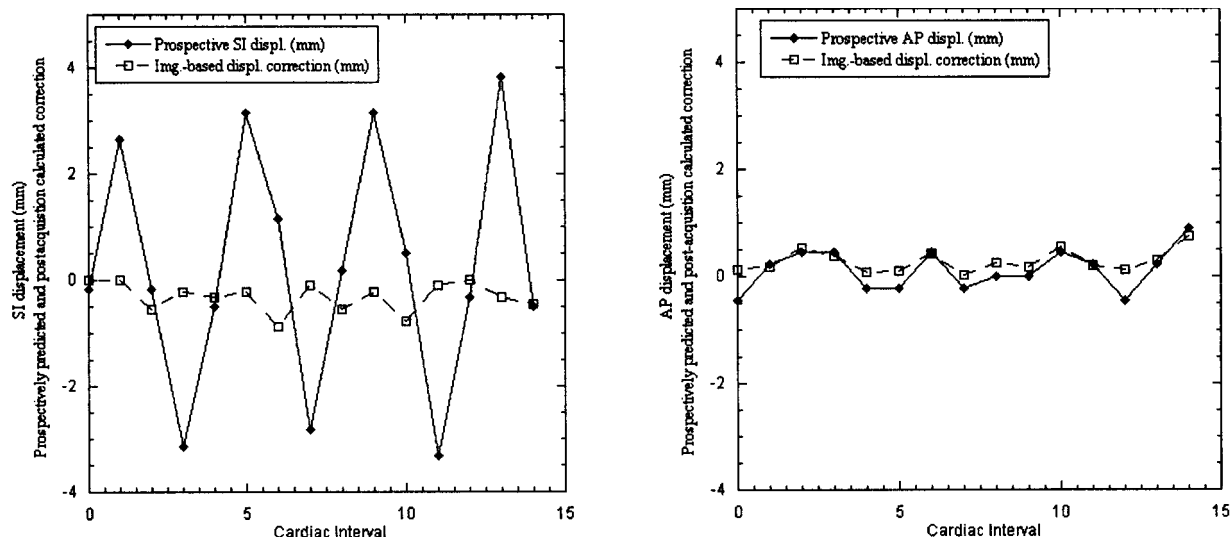


Figure 9. SI and AP motions as predicted by the navigators and displacement corrections needed, as per postprocessed, prospectively aligned images, for Case II.

images. Figure 7 shows the navigator-predicted displacement in the SI and the AP directions, along with the displacement correction suggested in both directions. The amplitude of the residual correction is ± 0.64 mm in SI and ± 0.52 mm in the AP direction.

In Case II (Fig. 8), a smaller field-of-view is considered, and the marker line again illustrates that the various organs are displaced over the various cardiac cycles, while the heart remains stationary. The respiratory displacements are smaller in this volunteer as compared with the volunteer in Case I.

Figure 9 shows the navigator-predicted displacement in the SI and the AP directions, along with the displacement correction suggested in both directions, for Case II. The amplitude of the residual correction is ± 0.28 mm in SI and ± 0.21 mm in the AP direction.

Both cases illustrate that the prospective implementation of RaMP navigators is able to predict, and correct for, the bulk motion of the heart over multiple cardiac cycles to within ± 1.43 mm in the SI direction and ± 0.84 mm in the AP direction.

CONCLUSION

The RaMP navigator is demonstrated to be a feasible method for tracking the bulk translational motion of the heart. It has been applied in the SI and AP direction to obtain heart displacement in both directions simultaneously. Unlike other prospective navigation schemes, it does not rely on empirical correlations between the

diaphragm and the heart. Also, RaMP navigators utilize small flip angles ($\alpha \leq 10^\circ$) so as to avoid interference with subsequent scans, while yielding sufficient SNR. For these reasons, the prospective version of the RaMP navigator is well-suited for cardiac scans that acquire uninterrupted time series of multiple, single-shot images, such as in function and perfusion assessments. However, RaMP navigators in coronary imaging needs to be further assessed by comparing it with other established navigator methods.

There are limitations to this navigating scheme. Some of these are outlined below:

1. By its very definition, RaMP navigation needs to obtain signal from moving blood to be successful in its implementation. So practical implementation of this approach of navigation may be nontrivial for pulse sequences, which require blood suppression or saturation.
2. Since RaMP depends on the signal from fast-moving blood volume, this navigation scheme has to be primarily applied in mid-systole or mid-diastole in order to maximize the navigation signal received, and these time frames may not be available for navigation in some exams. This may also lengthen the interval between the navigators and the image acquisition, thereby affecting the timeliness of the position measurement.
3. In conditions where the heart rate changes drastically, such as in stress imaging, the time of mid-systole or mid-diastole may also change significantly, causing the RaMP navigator to miss the rapid ejection/filling phase. Therefore, in such conditions it will be

necessary to dynamically adapt the timing of the RaMP navigator.

ACKNOWLEDGMENTS

We would like to acknowledge the assistance provided by Dr. U. Decking and Mr. E. Bennett at NIH, and Dr. R. Loeffler at Siemens Medical Systems for the implementation and testing of the RaMP sequence. We thank the reviewers for their helpful comments and suggestions. This research was funded by the NHLBI Division of Intramural Research.

REFERENCES

- Bland, J. M., Altman, D. G. (1986). Statistical methods for assessing agreement between two methods of clinical measurement. *The Lancet* February 8: 307–310.
- Bland, J. M., Altman, D. G. (1999). Measuring agreement in method comparison studies. *Stat. Met. Med. Res.* 8:135–160.
- Crawley, A. P., Henkelman, R. M. (1987). Errors in T2 estimation using multislice multiple-echo imaging. *Magn. Reson. Med.* 4:34–47.
- Danias, P. G., Stuber, M., Botnar, R. M., Kissinger, K. V., Edelman, R. R., Manning, W. J. (1999). Relationship between motion of coronary arteries and diaphragm during free breathing: lessons from real-time MR imaging. *AJR Am. J. Roentgenol.* 172:1061–1065.
- Duerinckx, A. J., Urman, M. K. (1994). Two-dimensional coronary MR angiography: analysis of initial clinical results. *Radiology* 193:731–738.
- Ehman, R. L., Felmlee, J. P. (1989). Adaptive technique for high-definition MR imaging of moving structures. *Radiology* 173:255–263.
- Haacke, E. M., Li, D., Kaushikkar, S. (1995). Cardiac MR imaging: principles and techniques. *Top Magn. Reson. Imaging* 7:200–217.
- Haase, A., Frahm, J., Matthaei, D., Hancic, W., Merboldt, R. D. (1986). FLASH Imaging. Rapid NMR imaging using low flip-angle pulses. *J. Magn. Reson.* 67:258–266.
- Hofman, M. B.M., Paschal, C. B., Li, D., Haacke, E. M., van Rossum, A. C., Sprenger, M. (1995). MRI of coronary arteries: 2D breath-hold vs. 3D respiratory-gated acquisition. *J. Comput. Assist. Tomogr.* 19:56–62.
- Johansson, L. O., Fischer, S. E., Smink, J., Hofman, M. B. M., Lorenz, C. H. (1998). Using real-time imaging to determine the correlation between the position of the heart and a navigator echo positioned on the diaphragm (abstr). In: Proceedings of the Sixth Meeting of the International Society for Magnetic Resonance in Medicine. Berkeley, Calif.: International Society for Magnetic Resonance in Medicine, p. 855.
- Keegan, J., Gatehouse, P., Yang, G. Z., Firmin, D. (2002). Coronary artery motion with the respiratory cycle during breath-holding and free-breathing: implications for slice-followed coronary artery imaging. *Magn. Reson. Med.* 47:476–481.
- Manning, W. J., Li, W., Edelman, R. R. (1993). A preliminary report comparing magnetic resonance coronary angiography with conventional contrast angiography. *N. Engl. J. Med.* 328:828–832.
- Meyer, C. H., Hu, B. S., Nishimura, D. G., Macovski, A. (1992). Fast spiral coronary artery imaging. *Magn. Reson. Med.* 28:202–213.
- Nagel, E., Bornstedt, A., Schnackenburg, B., Hug, J., Oswald, H., Fleck, E. (1999). Optimization of realtime adaptive navigator correction for 3D magnetic resonance coronary angiography. *Magn. Reson. Med.* 42:408–411.
- Nehrke, K., Bornert, P., Manke, D., Bock, J. C. (2001). Free-breathing cardiac MR imaging: study of implications of respiratory motion—initial results. *Radiology* 220(3):810–815.
- Oppelt, A., Graumann, R., Barfuss, H., Fischer, H., Hertl, W., Schajor, W. (1986). FISP: A new fast MRI sequence. *Electromedica* 54:15–18.
- Paling, M. R., Brookeman, J. R. (1986). Respiration artifacts in MR imaging: reduction by breath holding. *J. Comput. Asst. Tomogr.* 10:1080–1082.
- Pennell, D. J., Keegan, J., Firmin, D. N., Gatehouse, P. D., Underwood, S. R., Longmore, D. B. (1993). Magnetic resonance imaging of coronary arteries: techniques and preliminary results. *Br. Heart J.* 70: 315–326.
- Post, J. C., van Rossum, A. C., Hofman, M. B., Valk, J., Visser, C. A. (1995). Protocol for two-dimensional magnetic resonance coronary angiography studied in three-dimensional magnetic resonance data sets. *Am. Heart J.* 130:167–173.
- Sachs, T. S., Meyer, C. H., Hu, B. S., Kuhli, J., Nishimura, D. G., Macovski, A. (1994). Real-time motion detection in spiral MRI using navigators. *Magn. Reson. Med.* 32:639–645.
- Sakuma, H., Caputo, G. R., Steffens, J. C., O'Sullivan, M., Bourne, M. W., Shimakawa, A., Foo, T. K., Higgins, C. B. (1994). Breath-hold MR cine angiography of coronary arteries in healthy



- volunteers: value of multiangle oblique imaging planes. *AJR Am. J. Roentgenol.* 163:533–537.
- Stuber, M., Botnar, R. M., Danias, P. G., Kissinger, K. V., Manning, W. J. (1999). Submillimeter three-dimensional coronary MR angiography with real-time navigator correction: comparison of navigator locations. *Radiology* 212:579–587.
- Taylor, A. M., Jhooti, P., Keegan, J., Firmin, D. N., Pennel, D. J. (1998). Improved MR coronary angiography using real-time navigator echoes and a subject specific calculated adaptive motion correction factor (abstr). In: Proceedings of the Sixth Meeting of the International Society for Magnetic Resonance in Medicine. Berkeley, Calif.: International Society for Magnetic Resonance in Medicine, p. 322.
- Wang, Y., Riederer, S. J., Ehman, R. L. (1995). Respiratory motion of the heart: kinematics and the implications for the spatial resolution in coronary imaging. *Magn. Reson. Med.* 33:713–719.
- Wang, Y., Rossman, P. J., Grimm, R. C., Riederer, S. J., Ehman, R. L. (1996). Navigator-echo based real-time respiratory gating and triggering for reduction of respiration effects in three-dimensional coronary MR angiography. *Radiology* 198:55–60.

Received May 13, 2002

Accepted May 17, 2003

